Molecular Crystals and Liquid Crystals

ISSN: 1542-1406 (Print) 1563-5287 (Online) Journal homepage: http://www.tandfonline.com/loi/gmcl20

F^-/OH^- Triggered Optical Switching Functions of Naphthalimide Chromophoric Materials

Xiaochuan Li & Young-A. Son

To cite this article: Xiaochuan Li & Young-A. Son (2014) F^-/OH^- Triggered Optical Switching Functions of Naphthalimide Chromophoric Materials, Molecular Crystals and Liquid Crystals, 604:1, 184-192, DOI: 10.1080/15421406.2014.978569

To link to this article: http://dx.doi.org/10.1080/15421406.2014.978569

Published online: 15 Dec 2014.

Mole. Cryst. Liq. Cryst., Vol. 604: pp. 184–192, 2014

ISSN: 1542-1406 print/1563-5287 online
DOI: 10.1080/15421406.2014.978569

F^-/OH^- Triggered Optical Switching Functions of Naphthalimide Chromophoric Materials

XIAOCHUAN LI[1,2,*] AND YOUNG-A. SON[3,*]

[1]Collaborative Innovation Center of Henan Province for Green Manufacturing of Fine Chemicals, Key Laboratory of Green Chemical Media and Reactions, Ministry of Education, School of Chemistry and Chemical Engineering, Henan Normal University, Xinxiang, Henan, P. R. China
[2]Jiangxi Key Laboratory of Organic Chemistry, Jiangxi Science & Technology Normal University, Nanchang, P. R. China
[3]Department of Advanced Organic Materials Science and Engineering, Chungnam National University, Daejeon, S. Korea

Two naphthalimide based chemosensors were synthesized. Upon the addition of OH^- or F^-, the solution color turned from pink to blue due to the proton elimination of N-H/O-H. The electron density increased on the nitrogen atom and enhanced the intramolecular charge transfer, which resulted in a red-shift of the absorption band. This color change was reversible with H^+/MeOH addition and can be detected with the naked eye. The selectivity of the two dyes toward OH^-/F^- compared with other anions was investigated. The underlying signal mechanism was interpreted by the HOMO/LUMO potentials. Significantly lowered energy gap supported the red-shift absorption band.

Keywords Naphthalimide; chemosensor; spectral switching; charge transfer; HOMO/LUMO

Introduction

Colorful high-efficiency fluorophores have been intensively developed due to their highly sensitivity to external stimuli, which have the potential to significantly influence the development of numerous important materials science and structural biotechnologies [1–4]. This potential is singificantly advanced by various fluorophores [5–8]. 1,8-naphthalimide is one of the typical framework of fluorophore and has been widely used for various molecular designs, including fluorescent dyes [9–13], molecular probes [14–16], OLEDs [17], solar cells [18], liquid crystals [19], etc. Chemosensors that convert molecular recognition into highly sensitive and easily detectable signals have been actively investigated. To a large extent, the molecular design for chemsensors is based on the framework of 1,8-naphthalimide,

*Address correspondence to Prof. Xiaochuan Li, School of Chemistry and Chemical Engineering, Henan Normal University East Jianshe Rd. 46, Xinxiang, Henan 453007, China. E-mail: lixiaochuan@htu.cn and Prof. Young-A Son, Department of Advanced Organic Materials Engineering, Chungnam National University 220 Gung-dong, Daejeon 305-764, Korea. E-mail: yason@cnu.ac.kr

Color versions of one or more of the figures in the article can be found online at www.tandfonline.com/gmcl.

in which the photoinduced electron transfer (**PET**), photoinduced charge transfer (**PCT**) or fluorescence resonance energy transfer (**FRET**) mechanism is employed for the construction of various types of ion chemo-sensors. It has been well accepted in an abundance of published papers that the intramolecular **PET** and **PCT** are the most commonly exploited mechanisms to elucidate this remarkable physicochemical phenomena. With the presence of guest species, the nature of the output signal of the molecular system governed by **PET** or **PCT** can be finely modulated, which may lead to absorbance or emission changes.

The application of chemo-sensors has been widely used in various disciplines such as biochemistry [20], medical science [21], analytical chemistry [22], and the environmental sciences [23]. However, highly selective and sensitive sensors for cations, anions, and H^+/OH^- are still needed to develop the desirable requirements of the biological or chemical environment. Among various chemo-sensors, fluoride ions detection stands out and target for sensor design due to its smallest ionic radius, highest charge density and a hard Lewis basic nature [24]. Recent development of fluoride ions detection and the importance of fluoride ions in biological and medical process were reviewed in Chem. Rev. [25].

The molecular design of most naphthalimide based sensors is based on attaching an electron donor unit at the 4-position of the naphthalimide framework. Generally, amino, hydrazine, and piperidine are chosen as the electron donor unit to attach to the 4-position of naphthalimides. Protonation/deprotonation or binding with guest species occurs at the electron donor N atoms and can effectively influence the **PET** process and result in fluorescence "on/off' switching or color change. Condensation between deficient imide and other functional groups is another alternative for construction of Donor/Acceptor-Fluorophore-Acceptor type molecular systems [15, 26]. This construction may facilitate the modulation of the internal charge transfer from the fluorophore to the donor/acceptor with binding of the analyte (cation, anion, or H^+). The double direction of the photoinduced charge transfer process is closely related to the effect on optical characteristics, which are induced by electronic interactions between the naphthalimide and the donor/acceptor.

Experimental

Materials and Analysis

The solvents used in photochemical measurements were spectroscopic grade and further purified by distillation prior to use. The stock solution of compounds (2×10^{-3} M) was prepared in DMF and a fixed amount of their concentrated solutions was added to each experimental solution. NMR spectra were recorded on a Brucker Advance 400 spectrometer, operating at 400 MHz for proton and 100 MHz for carbon. The measurement was carried out in DMSO-d_6 solution. The chemical shifts (given as δ in ppm) were referenced to tetramethylsilane (TMS). Mass spectra were measured on an LC-MS (Waters120 QTof) mass spectrometer. High resolution mass spectra were measured on a Brucker microOTOF II Focus. Absorption spectra were measured with a PERSEE TU-1900 spectrophotometer. All experiments were carried out repeatedly and reproducible results were obtained. Prior to the spectroscopic measurements, solutions were deoxygenated by bubbling nitrogen through them.

Preparation and Characterization

All the solvents used in the reaction were of analytical grade and were dried according to the method described elsewhere [27]. 4-bromo-1,8-naphthalic anhydride was commercially available and purchased from Aldrich and was used for synthesis without further

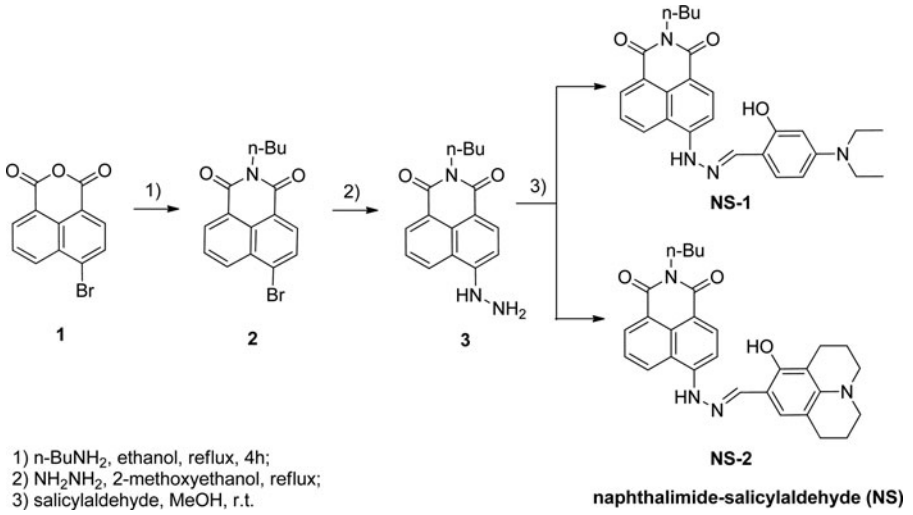

Scheme 1. Synthesis of naphthalimide-salicylaldehyde.

purification. Compound **2** (*N*-butyl-4-bromo-1,8-naphthalimide) was synthesized with the following procedure mentioned in the scheme described earlier [28]. The bromo atom attached at the 4-position of 1,8-naphthalimide was substituted by the nitrogen atom of the hydrazine hydrate and gave **3** (*N*-butyl-4-hydrazinyl-1,8-naphthalimide) [29].

General Procedure for the Synthesis of Naphthalimide-Salicylaldehyde (NS)

As shown in Scheme 1, to a magnetically stirred solution of compound **3** (71 mg, 0.25 mmol) in dry methanol (25 mL), salicylaldehyde (0.25 mmol) was added. Gradually, a red precipitate was generated. The mixture was stirred at room temperature for 24 h. The precipitate was collected by filtration and washed with MeOH. A pure sample was obtained by recrystallization using ethanol and this was dried in vacuum.

NS-1

Red solid, Yield 80% (92 mg); ^{1}H NMR (400 MHz, DMSO-d_6) δ 11.24 (s, 1H), 10.26 (s, 1H), 8.78 (d, $J = 8.2$ Hz, 1H), 8.61 (s, 1H), 8.46 (d, $J = 7.2$ Hz, 1H), 8.34 (d, $J = 8.5$ Hz, 1H), 7.74 (t, $J = 7.9$ Hz, 1H), 7.49 (d, $J = 8.8$ Hz, 1H), 7.42 (d, $J = 8.4$ Hz, 1H), 6.31 (d, $J = 7.6$ Hz, 1H), 6.17 (s, 1H), 4.02 (t, $J = 7.3$ Hz, 2H), 3.42 (s, 4H), 1.66 – 1.53 (m, 2H), 1.34 (dd, $J = 14.5$, 7.0 Hz, 2H), 1.13 (t, $J = 6.8$ Hz, 6H), 0.93 (t, $J = 7.3$ Hz, 3H); ^{13}C NMR (101 MHz, DMSO-d_6) δ 163.6, 162.8, 158.1, 149.9, 146.1, 145.2, 133.8, 130.7, 129.2, 129.1, 128.2, 124.6, 121.8, 118.4, 109.6, 107.4, 105.3, 104.1, 97.2, 43.8, 29.7, 19.7, 13.7, 12.5; MS (70 ev, EI): 458[M]$^+$. HRMS (70 ev, EI): $C_{27}H_{30}N_4O_3$ requires 458.2318; found 458.2315.

NS-2

Red solid, Yield 97% (95 mg); ^{1}H NMR (400 MHz, DMSO-d_6) δ 11.22 (s, 1H), 10.84 (s, 1H), 8.73 (d, $J = 8.9$ Hz, 1H), 8.45 (d, $J = 6.9$ Hz, 1H), 8.39 (s, 1H), 8.34 (d, $J = 8.3$ Hz, 1H), 7.75 (t, $J = 8.6$ Hz, 1H), 7.19 (d, $J = 8.7$ Hz, 1H), 6.76 (s, 1H), 4.01 (s, 2H), 3.18

(d, $J = 4.2$ Hz, 4H), 2.63 (d, $J = 4.7$ Hz, 4H), 1.87 (d, $J = 5.4$ Hz, 4H), 1.65 – 1.54 (m, 2H), 1.34 (dd, $J = 15.0, 7.4$ Hz, 2H), 0.92 (t, $J = 7.2$ Hz, 3H); ^{13}C NMR (101 MHz, DMSO-d_6) δ 163.6, 162.8, 153.5, 149.0, 145.4, 145.1, 133.8, 130.7, 129.2, 128.1, 127.8, 124.7, 121.9, 118.5, 112.9, 110.1, 106.2, 106.1, 104.9, 49.3, 48.8, 29.7, 26.5, 21.4, 20.6, 20.2, 19.7, 13.6. MS (70 ev, EI): 482[M^+]; HRMS (70 ev, EI): $C_{29}H_{30}N_4O_3$ requires 482.2318; found 482.2322.

Results and Discussion

NS-1 and **NS-2** showed an intense absorption peak around 500 nm ($\varepsilon_{NS\text{-}1} = 3.5 \times 10^4$ and $\varepsilon_{NS\text{-}2} = 1.4\times10^4$ $M^{-1}cm^{-1}$). This peak corresponds to the intramolecular charge transfer process of the nitrogen atom substituted naphthalimide moiety. The effects of deprotonation and protonation on colorimetric and chemosensing properties using a 2.0×10^{-5} M solution of **NS** in DMF were investigated. The titration spectra of OH^- for **NS-1** and **NS-2** are shown in Fig. 1, and a similar contour was observed between them. Upon addition of OH^-, the main absorption peak around 500 nm decreased and a new absorption peak appeared (605 nm for **NS-1**, 600 nm for **NS-2**). The isobestic points at 335, 384, 435, 540 nm for **NS-1** and 339, 374, 434, 535 nm for **NS-2** are clearly observed in Fig. 1, which indicates only two species co-exist in the equilibrium. The color of the **NS** solutions was gradually changed from pink to blue with the addition of OH^-. Before and after the addition of OH^-, no observable fluorescence emission changes were observed. The electron donation of shiff base unit caused **PET** to become competitively more viable and quenched the emission of naphthalimide. The quantum yield of **NS-1** and **NS-2** were lower than 0.1 in various solvents. The pink color of the solutions can be recovered by addition of H^+. This UV-vis absorption changes induced by OH^-/H^+ can be attributed to the deprotonation/protonation of the two dyes.

Upon the addition of F^- to the above DMF solutions, the spectral changes were the same as those for the OH^- addition. Fig. 2 shows the titration spectra of the F^- addition. The longest maximum absorption around 500 nm decreased and a new absorption band around 600 nm gradually increased with clear isosbestic points (332, 384, 434, 540 nm for **NS-1** and 331, 377, 432, 535 nm for **NS-2**). As a result, the color of the solutions turned from pink to blue. This color change can also be changed reversibly to pink with the addition of methanol, which provides protons. The deprotonation effect from amide NH group and OH group was also demonstrated. Responses to various metal cations for **NS-1** and **NS-2** were also investigated. However, no obvious color or fluorescence emission changes were observed. The experimental result is different from a literature report regarding a similar structure [30]. The electron donor attached to the benzene ring enhances the **PCT** process and results in the low quantum yield of **NS**. This is different from the higher fluorescent structure in the reference [30]. Even if metal cations can interact with **NS**, the ability of metal cations was lost with no fluorescence or color signal input.

Fig. 3 depicts the remarkably selectivity of **NS-1** and **NS-2** towards F^- over other anions. The absorption of **NS** showed a weak response with other anions such as Cl^-, Br^-, I^-, SO_4^{2-}, NO_3^-, $H_3PO_4^-$, CO_3^{2-}, ClO_4^-, and Ac^-. The highly selective binding property of **NS** toward F^- was attributed to the strong Lewis base property of F^-. It is also worth noting that deprotonation occurred with OH^- or F^- addition and can result in the capture of two protons from N-H and O-H. The proposed binding mode is shown in Scheme 2. The occurrence of deprotonation from N-H and O-H by OH^-/F^- additiion resulted a significant increasing of the electron density on the nitrogen and oxygen atoms. The negative charge may be delocalized on the oxygen atom of the imide, which results in enhancement of

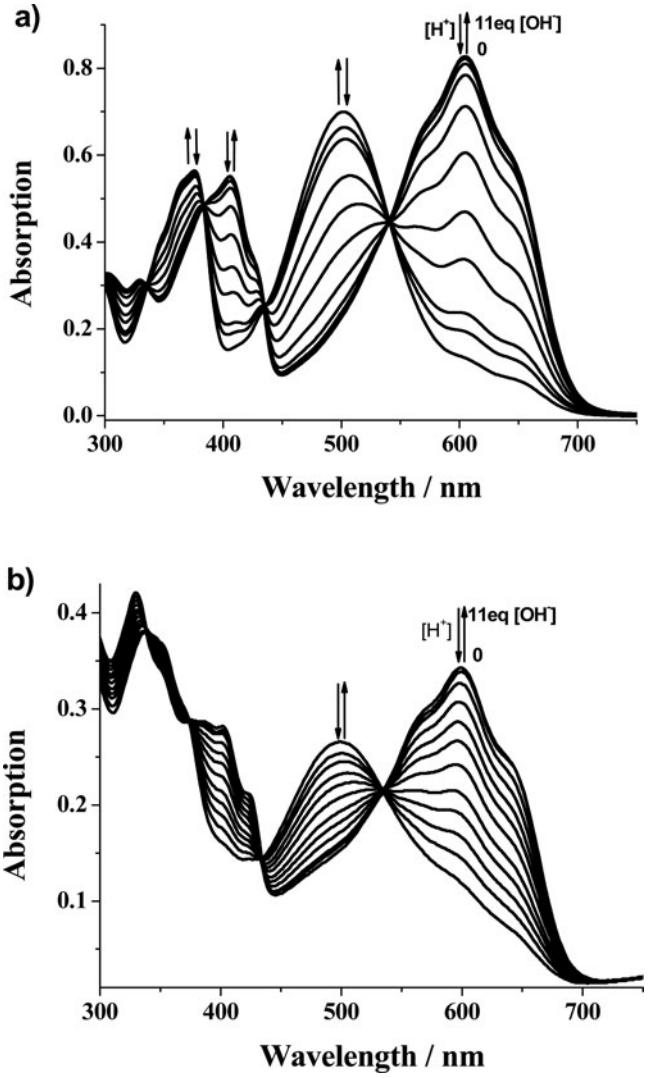

Figure 1. Absorption change of **NS** in DMF solution (2.0×10^{-5} M) by addition of OH^- and H^+.

the **PCT** process and a red-shift of the **PCT** absorption band. The resonance structures (**NS-a/NS-b**) indicate delocalization of the negative charge from the nitrogen atom to the oxygen atom.

In order to gain further insight into the geometrical, electronic and optical properties of **NS**, **NS-1** as a representative compound was investigated in detail using quantum chemistry. The geometric structure was computationally optimized with density functional theory (DFT) with GGA/BLYP set in *Dmol*^{3} package [31, 32]. No higher level of calculation was deemed necessary, considering the purpose was to compare properties of the molecules. The size and sign of the highest occupied molecular orbital (HOMO) and the lowest unoccupied molecular orbital (LUMO) are illustrated in Fig. 4 with the charge transfer operation. It is apparent that the electron density of **NS-1** was distributed over the N-substituted benzene ring in HOMO, whereas that of the LUMO was localized away from the benzene ring to the

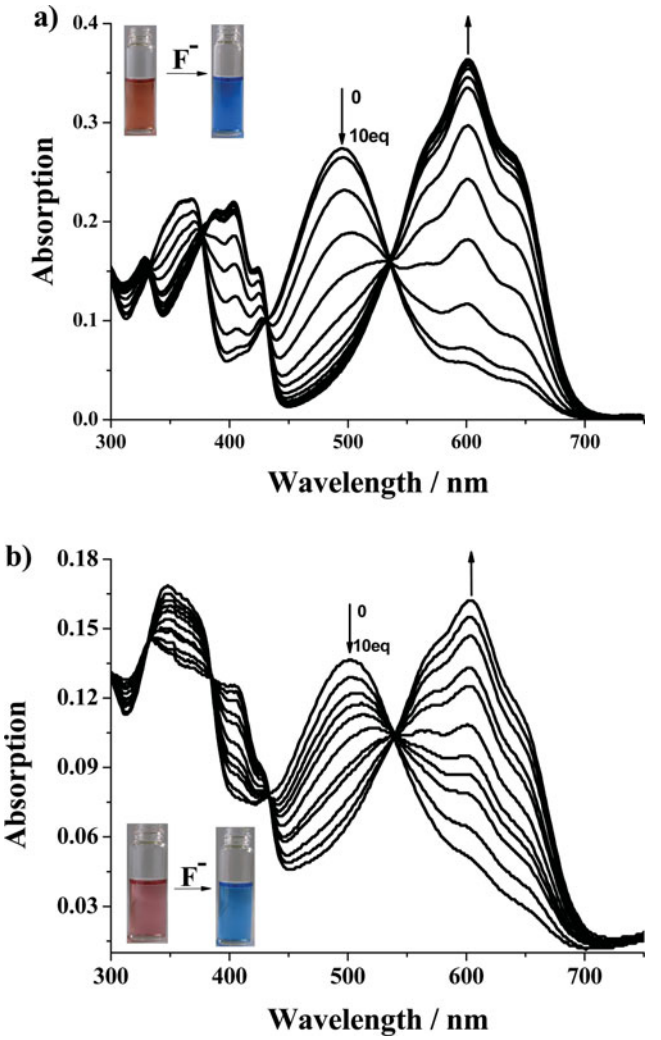

Figure 2. Changes in the UV-vis absorption spectra of **NS-1** and **NS-2** with F^- addition in DMF (0–10 eq).

naphthalene ring. Once the protons of N-H and O-H were captured by F^-/OH^-, the electron density of the nitrogen atoms between the naphthalene ring and the benzene ring increased in the HOMO. Part of the electron density was distributed to the naphthalene ring. In the LUMO state of **NS-1a**, most of the electron density was spread over the naphthalene ring and the nitrogen atoms. The elimination of a proton resulted in the electron distribution to naphthalene in advance and enhanced the effect. The resonance hybrid (**NS-1a** and **NS-1b**) has an identical electron distribution according to the quantum calculation. The energy levels of HOMO/LUMO of **NS-1**, **NS-1a**, and **NS-1b** were calculated. E_{HOMO} of **NS-1a** (−0.117 eV) greatly increased with respect to E_{HOMO} of **NS-1** (−0.168 eV). E_{LUMO} of **NS-1a** (−0.076 eV) also increased with respect to E_{LUMO} of **NS-1** (−0.108 eV). According to the characteristics of the HOMO/LUMO states of **NS-1** and **NS-1a**, the effect of the first deprotonation may contribute much more to the red-shift of the absorption band. The lowest

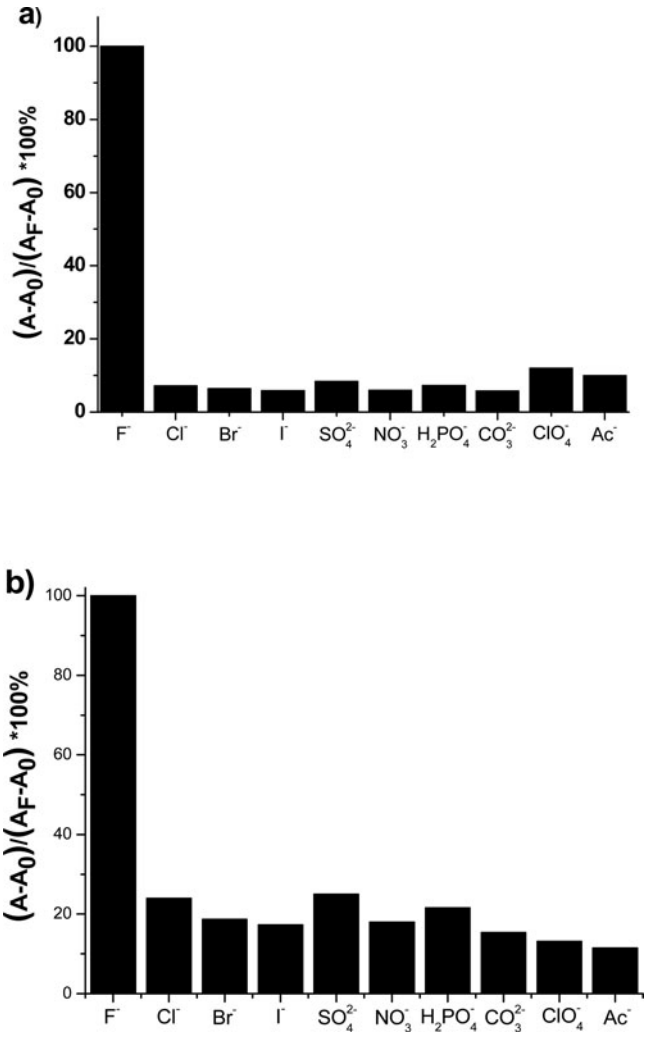

Figure 3. Comparison of percent increase of absorption of **NS-1** and **NS-2** in DMF solution at 600 nm in the presence of 10 equivalents of various anions.

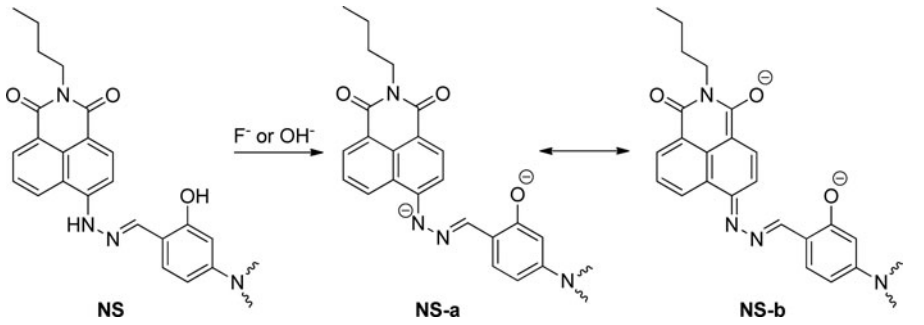

Scheme 2. Concept of deprotonation by F^- and OH^-.

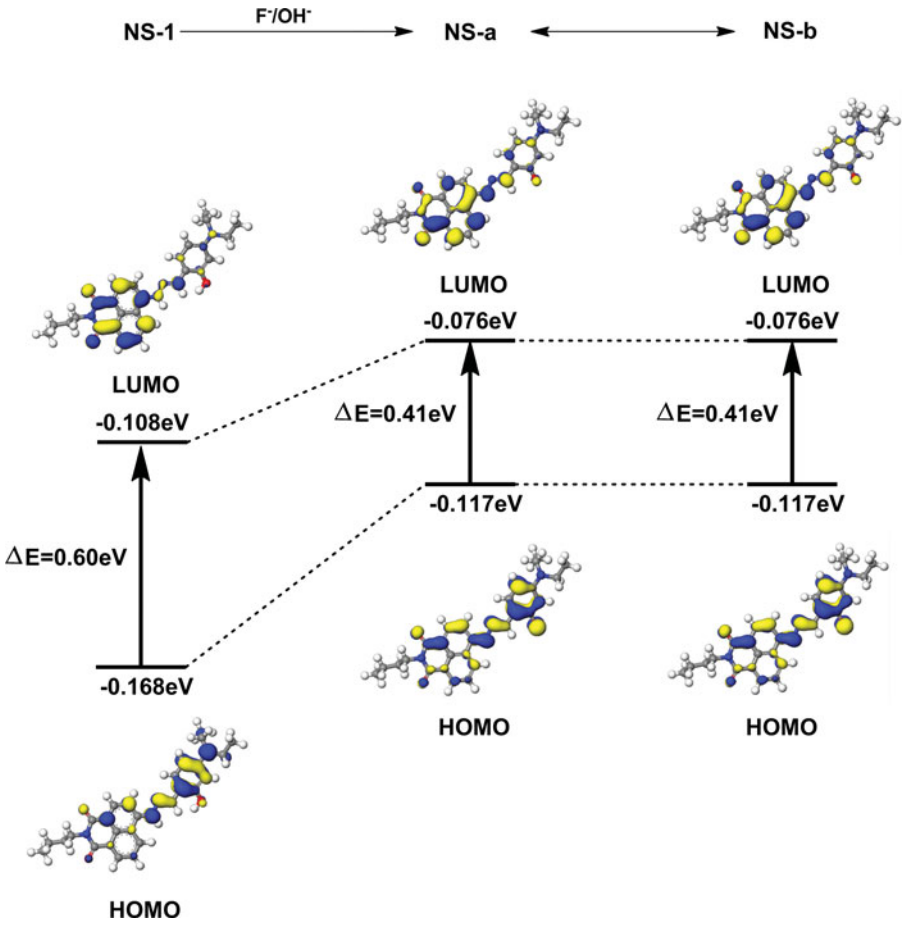

Figure 4. Electron distribution of HOMO and LUMO energy levels of **NS.**

excitation energy gap was lowered from 0.60 to 0.41 eV with before and after elimination of the proton, which agreed well with the observed maximum absorption wavelengths. That is, the absorption band decreased at 500 nm and new absorption band increased at 600 nm.

In summary, two new naphthalimide-salicylaldehyde dyes were synthesized and fully characterized. The deprotonation/protonation effects were investigated in detail with OH^-/H^+ and F^-/MeOH addition. Upon addition of OH^- or F^-, the absorption centered at 500 nm decreased and a new absorption band centered at 600 nm increased. With the addition of OH^- or F^-, the solution color turned from pink to blue. The occurrence of N-H and O-H deprotonation resulted in an obvious increase of electron density on the corresponding nitrogen atom. This finding was supported by calculation of the HOMO and LUMO. The energy gap evaluated by quantum calculations for **NS-1**, **NS-1a**, and **NS-1b** fitted well with the experimental photo-physical properties.

Funding

This work was supported by the National Natural Science Foundation of China (Grant no. 21272060) and Jianxi Key Lab of Organic Chemistry (Grant no. GFZ-KF-201301). This

study was supported by Basic Science Research Program through the National Research Foundation of Korea (NRF) funded by the Ministry of Science, ICT and Future Planning (Grant no. 2014006660).

References

[1] Yuan, L., Lin, W., Zheng, K., & Zhu, S. (2013). *Chem. Rev.*, *46*, 1462.
[2] Yang, Y., Zhao, Q., Feng, W., & Li, F. (2013). *Chem. Rev.*, *113*, 192.
[3] Li, X., Ma, Y., Wang, B., & Li, G. (2008). *Org. Lett.*, *10*, 3639.
[4] Li, X., Xu, Y., Wang, B., & Son, Y.-A. (2012). *Tetrahedron Lett.*, *53*, 1098.
[5] Loudet, A., & Burgess, K. (2007). *Chem. Rev.*, *102*, 4891.
[6] Frath, D., Massue, J., Ulrich, G., & Ziessel, R. (2014). *Angew. Chem. Int. Ed.*, *53*, 2290.
[7] Li, X., & Son, Y.-A. (2014). *Dyes Pigments*, *107*, 182.
[8] Li, X., Kim, H., & Son, Y.-A. (2009). *Dyes Pigments*, *82*, 293.
[9] Li, Y., Cao, L., & Tian, H. (2006). *J. Org. Chem.*, *71*, 8279.
[10] Shakia, H., Gharanjiga, K., Rouhania, S., & Khosravib, A. (2010). *J. Photochem. Photobiolo. A: Chem.*, *216*, 44.
[11] Bardajee, G. R., Li, A. Y., Haley, J. C., & Winnik, M. A. (2008). *Dyes Pigments*, *79*, 24.
[12] Li, X., Zhu, K., Li, Y., Kim, H., & Son, Y.-A. (2013). *Mol. Cryst. Liq. Cryst.*, *584*, 18.
[13] Li, X., Zhu, K., Jiang, W., Li, Y., Kim, H., & Son, Y.-A. (2012). *Phys. Status Solidi C*, *9*, 2456.
[14] Wang, P., Liu, J., Lv, X., Liu, Y., Zhao, Y., & Guo, W. (2012). *Org. Lett.*, *14*, 520.
[15] Zhang, J. F., Kim, S., Han, J. H., Lee, S.-J., Pradhan, T., Cao, Q. Y., Lee, S. J., Kang, C., & Kim, J. S. (2011). *Org. Lett.*, *13*, 5294.
[16] Zhang, J. F., Lim, C. S., Bhuniya, S., Cho, B. R., & Kim, J. S. (2011). *Org. Lett.*, *13*, 1190.
[17] Kolosov, D., Adamovich, V., Djurovich, P., Thompson, M. E., & Adachi, C. (2002). *J. Am. Chem. Soc.*, *124*, 9945.
[18] Huang, X., Fang, Y., Li, X., Xie, Y., & Zhu, W. (2011). *Dyes Pigments*, *90*, 297.
[19] Hasharoni, K., Levanon, H., Greenfield, S. R., Gosztola, D. J., Svec, W. A., & Wasielewski, M. R. (1996). *J. Am. Chem. Soc.*, *118*, 10228.
[20] Mbatia, H. W., & Burdette, S. C. (2012). *Biochemistry*, *51*, 7212.
[21] Ott, I., Qian, X., Xu, Y., Vlecken, D. H. W., Marques, I. J., Kubutat, D., Will, J., Sheldrick, W. S., Jesse, P., Prokop, A., & Bagowski, C. P. (2009). *J. Med. Chem.*, *52*, 763.
[22] Lacivita, E., Leopoldo, M., Masotti, A. C., Inglese, C., Berardi, F., Perrone, R., Ganguly, S., Jafurulla, M., & Chattopadhyay, A. (2009). *J. Med. Chem.*, *52*, 7892.
[23] Xiong, L., Feng, J., Hu, R., Wang, S., Li, S., Li, Y., & Yang, G. (2013). *Anal. Chem.*, *85*, 4113.
[24] Ashokkumar, P., Weißhoff, H., Kraus, W., & Rurack, K. (2014). *Angew. Chem. Int. Ed.*, *53*, 2225.
[25] Zhou, Y., Zhang, J. F., & Yoon J. (2014). *Chem. Rev.*, *114*, 5511. And references cited there in.
[26] Pasis, V. F., Remon, P., Collado, D., Andreasson, J., Perez-Inestrosa, E., & Pischel, U. (2011). *Org. Lett.*, *13*, 5572.
[27] Vogel, A. I. (1994). *Textbook of Practical Organic Chemistry*. Singapore Publishers Ltd., Singapore.
[28] Wang, J., Xu, Z., Zhao, Y., Qiao, W., & Li, Z. (2007). *Dyes Pigments*, *74*, 103.
[29] Gan, J., Tian, H., Wang, Z. H., Chen, K. C., Hill, J., Lane, P. A., Rahn, M. D., Fox, A. M., & Bradley, D. D. C. (2002). *J. Organomet. Chem.*, *645*, 168.
[30] Yang, H., Song, H., Zhu, Y., & Yang, S. (2012). *Tetrahedron Lett.*, *53*, 2026.
[31] Lee, C., Yang, W., & Parr, R. G. (1988). *Phys. Rev. B*, *37*, 786.
[32] Becke, A. D. (1988). *J. Chem. Phys.*, *88*, 2547.